

Chemisorption of Atomic Oxygen on Pt(111) from DFT Studies of Pt-Clusters

Timo Jacob, Richard P. Muller, and William A. Goddard, III*

*Materials and Process Simulation Center (139-74), California Institute of Technology, Pasadena, California 91125**Received: June 5, 2003*

Using density functional theory (DFT) with gradient-corrected exchange-correlation functionals (B3LYP), we systematically study the electronic structure and bonding of oxygen to various Pt-clusters. Our aim is to understand how the cluster size and shape affect the chemistry of dispersed catalysts and to find the smallest cluster suitable for modeling surface reactions on the Pt(111)-surface. We find that the dependence of binding on the sites of these clusters is well described in terms of the interstitial electron model (IEM). The results show that the 28-atom three-layer Pt_{9,10,9}-cluster gives a good representation of the Pt(111)-surface for various adsorption sites. These results indicate that an O atom binds most strongly to the 3-fold hollow site with a binding energy of 3.28 eV for fcc and 2.95 eV for hcp. The binding energies for the other sites are 2.73 eV (bridge) and 2.02 eV (on-top). A one-layer 12-atom cluster does well at describing the bonding for all sites except the hcp site. These cluster results agree well with experimental results and with the best calculations on this surface: all results agree that the η_3 -fcc site is favored with a bond distance ≈ 2.01 Å. In addition, our calculated bond energy of 3.28 eV is consistent with experiment at low coverage (3.43 to 3.71 eV) and with the best DFT calculations on a surface (3.43 eV). We interpret the bonding of O to the η_3 sites (both fcc and hcp) in terms of the IEM localized covalent bonding model, in which the two singly occupied orbitals of O bond to singly occupied d orbitals of Pt, and the lone pair of p orbitals on the O coordinates to the third Pt of an η_3 site to form a donor–acceptor bond. This leads to two bonds of 2.01 Å and one of 2.21 Å.

1. Introduction

Despite enormous progress in the experimental study of chemisorption and reactions on metal surfaces, there remains much uncertainty regarding the detailed reaction mechanisms of many important processes on these surfaces. In particular, for electrocatalytic processes that occur in fuel cells, it has been difficult to characterize intermediate species involved in reactions such as the reduction of O₂ at the cathode. Furthermore, although much progress has been made in developing and applying improved theoretical methods to describe chemisorbed intermediates on metal surfaces, little has been done to characterize the processes in electrocatalytic systems, particularly with regard to the kinetics (barriers) of these processes.

For the quantum mechanical description of surfaces, two major approaches have been used:

(i) The slab/supercell approach. Here the 2-D periodic semi-infinite solid is approximated with a finite-thickness 2-D periodic slab. The thickness must be large enough that the surfaces are not affected by each other. If there is interest in describing chemical reactions on the surface, the 2-D cell must also be large enough that the adsorbed species involved in a reaction in one cell do not see their images in adjacent cell. This approach is most suitable for comparing to experiments involving ordered overlayers, but it may not be suitable for highly dispersed catalysts, which could have as few as 10–30 atoms.

(ii) The cluster-approximation approach. Here a cluster finite in all three directions is used to describe the processes on the surface, allowing one to analyze more easily how the local

electronic structure of a system affects the nature of chemisorption and reactive processes on surfaces. However, the cluster of atoms must be chosen to mimic the relevant sites for the chemistry of interest. This approach is most suitable for highly dispersed catalysts, where the number of atoms in the active catalyst particle can be as low as 10–30. The cluster approach may not be so useful for comparing to experiments involving ordered overlayers.

For semiconductor and insulator systems, it has been practical to study surface reactions using both periodically infinite 2-D slabs and finite clusters. Here the slabs have been useful for comparison to experiments on ordered overlayers and both approaches (periodic and cluster) have been useful in examining details of the reaction mechanism. Cluster approximations can provide a good description of surface reactions because the surface states tend to be fairly localized (with penetration into the bulk dropping off at a rate related to the band gap). Part of the slow progress in describing processes at metallic surfaces is caused by the delocalization of the valence electrons characteristic of metals, which suggests that very thick slabs may be required. Consequently, it is uncertain how well finite clusters (and thin slabs) can describe reactions on these surfaces.

Because of its importance for catalysis there have been numerous experimental and theoretical investigations on the Pt(111)-surface. Most theoretical studies on the chemisorption of an oxygen atom on Pt-surfaces have used clusters with up to about 10 atoms.^{1–3} Anderson and Grantscharova used a two-layer cluster consisting of 18 atoms to study reactions of CO and OH on Pt-surfaces.^{4,5} Kua⁶ used a single-layer cluster with eight or twelve atoms to study the chemisorption and decomposition of hydrocarbons and methanol. But there have also been calculations on periodic slabs (see section 3.4).

* Author to whom correspondence should be addressed. E-mail: wag@wag.caltech.edu.

The focus in this paper is to determine a suitable cluster for studying surface reactions of organic molecules on Pt(111). We have systematically increased the number of cluster atoms and have examined both the electronic structure of the cluster and the reactions with an O atom. We chose to examine chemisorption of oxygen because it makes a very strong bond that strongly perturbs the electronic structure of the Pt-clusters. Thus, a cluster that properly describes the chemisorption of oxygen is likely to be adequate for other surface processes involving organic fragments. We find that the orbital structure of the Pt-surface and its reactivity with an oxygen atom are consistent with the interstitial electron model (IEM).^{7,8}

Experimental studies on the adsorption of atomic oxygen on Pt(111) tend to agree that it is most favorable at 3-fold hollow sites, but the reported adsorption energies vary over a wide range from 2.16 to 5.20 eV.^{3,9–14} This is due to the coverage dependence and different experimental techniques. However, all measurements agree that low coverages lead to higher binding energies, since there is less O–O interaction.

There is good agreement on the bond distance and the vibrational frequency of the adsorbate:^{10,15–17} $R_{\text{S-O}} = 1.21 \pm 0.03$ Å for the surface-oxygen distance, which leads to $R_{\text{Pt-O}} = 2.01 \pm 0.05$ Å for the distance to the nearest Pt-atoms. The experimental surface vibrational frequency is $\omega_{\text{Pt-O}} = 466\text{--}480$ cm^{−1}. The theoretical DFT studies^{18–20} give bond distances and vibrational frequencies close to the experimental values. Both, the experimental and the theoretical results will be discussed in the sections 3.3 and 3.4.

2. Theoretical Methods

Our calculations were performed using spin-unrestricted density functional theory (DFT) with the gradient-corrected B3LYP GGA-functional (generalized gradient approximation).^{21,22} B3LYP combines exact Hartree–Fock (HF) exchange with the Slater²³ local exchange functional. In addition, it uses the Becke gradient correction,²⁴ the local Vosko–Wilk–Nusair exchange functional,²⁵ and the Lee–Yang–Parr local gradient-corrected functional.²²

We use B3LYP for these studies because of the established accuracy for the thermochemistry of organic molecules. This will be important in using these methods to examine the mechanisms for rearrangements and reactions of organics on Pt-surfaces. Since most calculations of bulk metal systems have used functionals that do not include exact exchange, we also evaluated the influence of using a density functional that includes exact exchange for metallic platinum. Therefore we repeated the calculation for O on Pt_{5,10,5} at the fcc site with the BLYP functional, which does not include HF exchange. We find that the BLYP functional gives an adsorption energy of 4.151 eV, in good agreement with 4.208 eV obtained with B3LYP.

We also tested the recently developed the X3LYP functional²⁶ in which the Becke GGA functional was modified to accurately describe van der Waals interactions. Using the X3LYP functional leads to 4.163 eV, indicating that the well-known problem of Becke functionals for treating dispersion is not a problem for O/Pt.

All ab initio calculations were carried out with the Jaguar program suite.²⁷ For the Pt-atoms, the 60 core electrons (1s–4f) were described using the Hay and Wadt core–valence relativistic effective-core potential (ECP) which leaves 18 valence electrons (the atomic ground state is (5s)²(5p)⁶,

(5d)⁹(6s)¹(6p)⁰).²⁸ This ECP uses angular momentum projection operators (i.e., it is a nonlocal ECP) to enforce the Pauli principle.^{29–32} In the Jaguar program this ECP is used in conjunction with the LACVP** basis set. For the oxygen atom, all electrons were treated explicitly using the 6-31G** basis set (5 functions for each d set). We assumed that at equilibrium additional diffuse functions on the oxygen cause minor effects. To prove this assumption, we also checked the influence of additional diffuse functions for the adsorption of oxygen at the fcc-site of the Pt_{5,10,5}-cluster (see section 3.2.1). The change in the energetics was only ≈ 0.015 eV, and the difference in charge transfer to the oxygen was ≈ 0.02 e.

The net spin density that is used in the discussion about the bond behavior and in Figure 7 is the difference between the spin densities for spin-up and spin-down as obtained from the Mulliken population.

3. Results and Discussion

3.1. Platinum-Clusters. Before calculating the adsorption of oxygen on the Pt-clusters, we calculated the electronic states of the bare clusters. We systematically examined clusters ranging in size from 3 to 28 atoms as shown in Figure 1: Pt₃, Pt₆, Pt₈, Pt₁₂, Pt_{6,3}, Pt_{8,4}, Pt_{12,7}, Pt_{5,10,5}, and Pt_{9,10,9}. The indices indicate the number of atoms per layer. For example, Pt_{12,7} denotes 12 atoms in the first and 7 atoms in the second layer. Because our aim is to simulate the Pt(111)-surface that has nearly no relaxation,³³ we fixed the distance between the Pt-atoms to the bulk value of 2.775 Å.

In choosing these clusters, we made use of the results from Kua and Goddard (hereafter KG),⁸ who systematically examined Pt-clusters up to about 12 atoms. Using the Interstitial Electron Model (IEM) introduced by McAdon and Goddard,⁷ KG were able to predict the spin-states for these clusters, which led to insights into the nature and locations of the orbitals in the metallic clusters and was used to predict preferred adsorption sites.

For each cluster, we calculated the ground state and the lowest energy states of varying spin multiplicity (see Table 1). As with KG, we considered all likely spin states and orbital occupations, by repeatedly exciting electrons from the higher occupied to lower empty orbitals. (Some of the smaller clusters were also calculated by Kua,⁸ but we recalculated these using the newest version of the Jaguar program to be internally consistent.)

Comparison of the energy differences between the states can be done for the smallest cluster Pt₃. Performing CASMCSF (complete active space multiconfiguration self-consistent field), MRSDCI (multireference singles and doubles configuration interaction), and DFT calculations without any spin–orbit effects, Balasubramanian et al.³⁴ found the singlet state to be most stable. However using RCI (relativistic configuration interaction) calculations, which include spin–orbit effects, he found the triplet state to be most stable, with the singlet state 0.078 eV higher. In our calculations on Pt₃ we also find the $S = 1$ state to be most stable, and find the excitation energy to the singlet state is 0.047 eV.

According to the IEM, the ground-state spin of a cluster can be predicted by the following procedure: Determine the number of interstitial bond orbitals (IBO) (primarily combinations of s-like orbitals that are localized in tetrahedral hollow sites) and occupy each of them with two electrons. All other electrons occupy d-orbitals. Assuming that the width of the d band is small compared to the intra-atom exchange energies, we expect

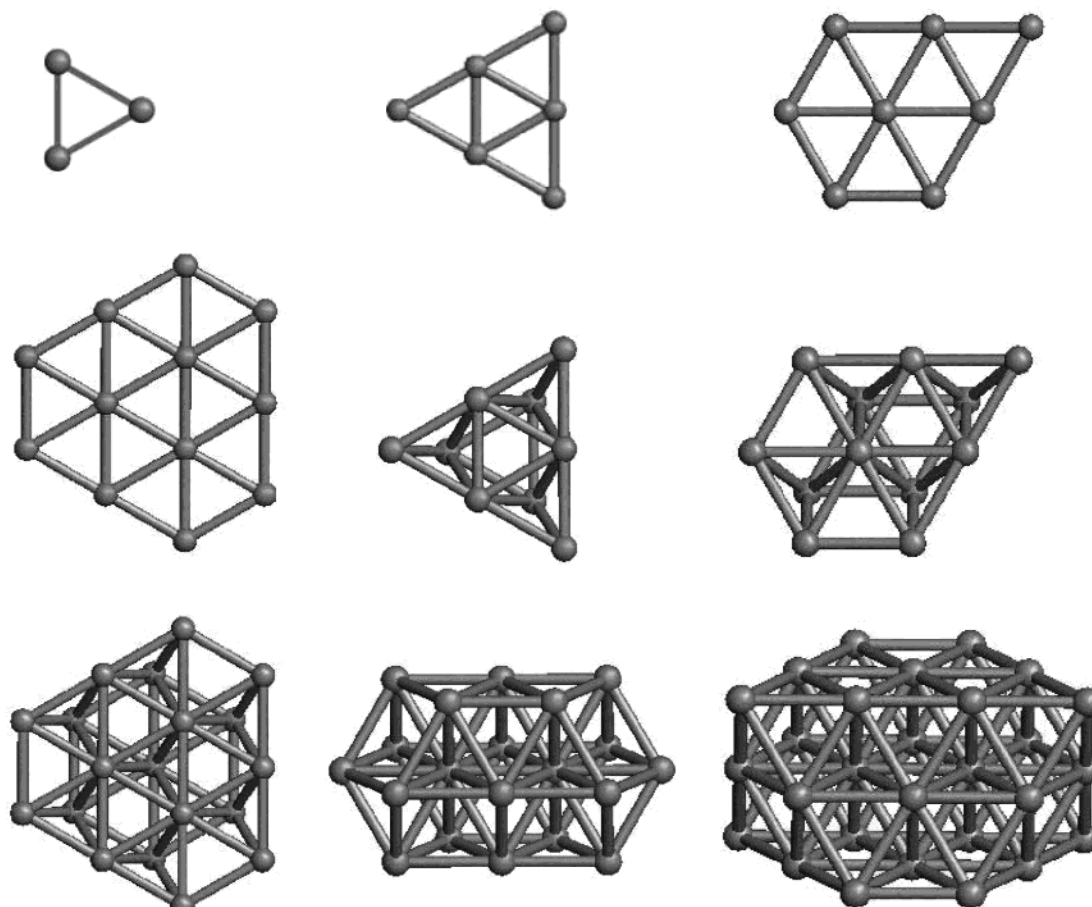


Figure 1. The figure shows the different one-, two-, and three-layer Pt-clusters without adsorbate: Pt₃, Pt₆, Pt₈, Pt₁₂, Pt_{6,3}, Pt_{8,4}, Pt_{12,7}, Pt_{5,10,5}, and Pt_{9,10,9}. All clusters are shown from the top.

and find that the ground-state spin will nearly always satisfy Hund's rule (maximum number of unpaired spins). For example, Pt_{6,3} has 4 IBOs that are located in the outermost tetrahedra and the face of the octahedron. Therefore 8 of the 90 valence electrons are in the IBOs (*s*-like orbitals), but the remaining 82 electrons occupy the $9 \times 5 = 45$ *d*-orbitals. The combination giving the highest spin-state consists of 45 spin-up and 37 spin-down electrons. This leads to a total spin-state of $S = 4$ (8 extra up-spin-orbitals). We find that this IEM-based model also correctly predicts the ground-state spin of the larger clusters. As the clusters get bigger, the width of the singly occupied states increases, so that sometimes a slightly lower spin state becomes more stable. However, such cases should always be close to the IEM-predicted spin. Since the smaller clusters were discussed by KG,⁸ we will discuss consistency of the IEM only for the larger systems.

For the planar 12-atom cluster Pt₁₂, there are two possibilities for placing IBOs in the surface triangles, which are shown in Figure 2a. In this figure the seven white circles show the first possibility and the six filled circles show the other way to locate the IBOs. Because of repulsive interactions between the IBOs (a combination of the Pauli principle and Coulomb repulsion), the system with fewer IBOs (6) is lower in energy. Our calculations find that the $S = 5$ state having 6 IBOs is 0.006 eV lower. However, $S = 5$ arises from spin pairing of the *d* electrons in the two highest *d*-like orbitals of $S = 6$ (Hund's rule not quite satisfied). Thus the system has 59 up- and 49 down-spin electrons. This is in agreement with the expectation of KG that such violations of Hund's rule occur more in larger clusters.

For the two-layer clusters, there may be several ways to distribute the IBOs. The number of IBOs and the positions are determined by the following: (1) some IBOs are between the two layers rather than in the surface plane; (2) IBOs prefer tetrahedra spaces rather than octahedra; (3) IBOs prefer not to occupy neighboring tetrahedra that share faces. This finally leads to a s^1d^9 electronic configuration for the Pt-surface. Since every Pt unit cell (fcc) has 4 Pt-atoms and 8 tetrahedra, one IBO corresponds to every Pt-atom (10 valence electrons) leading to a s^2d^8 configuration in the bulk. This was also found by angle-resolved ultraviolet photoemission spectroscopy (ARUPS).³⁵

For Pt_{12,7}, the application of these criteria predicts the 7 IBOs shown in Figure 2b. This would suggest a high spin ground state of $S = 7$. Although the $S = 6$ state (also with 7 IBOs) is 0.003 eV lower in energy, we assume the IEM prediction to be correct (see discussion about Pt₁₂).

The extension to three layers changes the electron configurations drastically. Whereas the positions of the IBOs in the two-layer clusters are mostly determined by the tetrahedra, the Pt_{5,10,5}- and Pt_{9,10,9}-clusters show more complex behavior. Since the clusters are finite, we must consider various orientations of the surface planes to determine the best configuration. Model c of Figure 2 shows the 20-atom system, which has 5 atoms in the first and third layers. Here the face on the right side also consists of 5 atoms and is symmetry-equivalent to the first layer. The same holds true for 5 atoms of the third layer. This equivalence of various surfaces leads to cluster orbitals that are more delocalized than in the two-layer clusters. We find a ground-state spin of $S = 5$, corresponding to 5 IBOs and the number of atoms in the first and third layers.

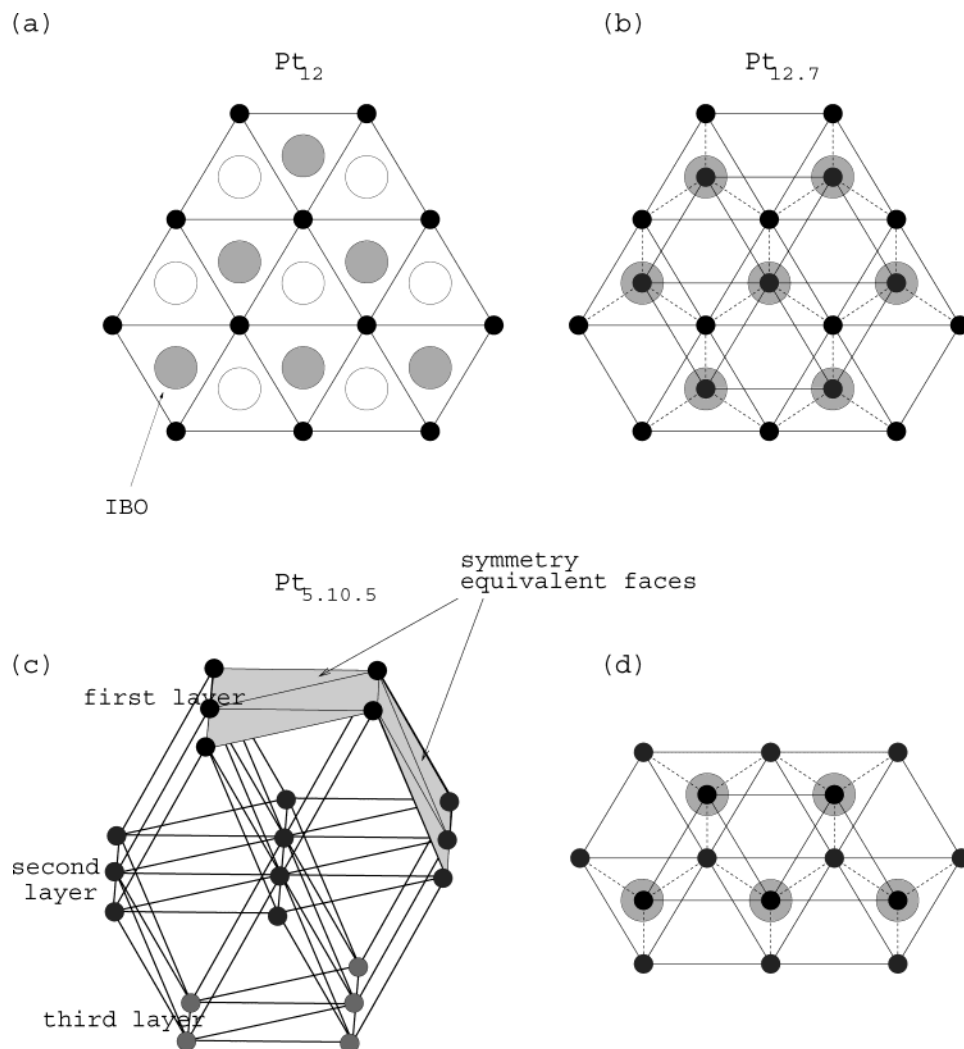


Figure 2. Distribution of the interstitial bond orbitals for different examples: (a) two possible (white and gray circles) distributions for the Pt_{12} -cluster. The gray arrangement (6 IBOs) leads to the calculated ground state, (b) $Pt_{12.7}$ (black dots are the first layer, gray dots the second layer) with its 7 IBOs, (c) $Pt_{5.10.5}$ with two of the four symmetry equivalent 5 atomic faces, (d) top-view of the first two layers of the $Pt_{5.10.5}$ -cluster. The IBOs are located at the five shown tetrahedra.

The enlarged 28-atom system $Pt_{9.10.9}$ also shows more complex symmetry than the two-layer clusters, leading to a ground-state spin of $S = 9$ corresponding to nine IBOs, again the number of atoms in the first and third layers. To check the generality of this result, we also calculated $Pt_{12.12.12}$ with 12 atoms in the first and third layers. This also leads to a ground-state spin value of $S = 12$, corresponding to the expected 12 IBOs. For these three-layer systems the IBOs are delocalized within symmetry-equivalent tetrahedra, leading to a spin-state that is exactly half of the total number of tetrahedra that could be occupied by IBOs. For example, Figure 2d shows the first and second layers of $Pt_{5.10.5}$. The IEM model would suggest that there could be 5 IBOs in the corresponding tetrahedra. However, there are also 5 additional tetrahedra involving only atoms of the second and third layers. Because of the symmetry, there are only 5 symmetry-inequivalent tetrahedra. According to the assumption mentioned above, this leads to a ground-state spin for this cluster of $S = 5$ (5 IBOs, see Figure 3). This is exactly the calculated value.

That these 20 and 28 atom clusters should be the smallest ones suitable for mimicking chemisorption on surfaces was suggested by Upton and Goddard in 1978,^{36–39} who reported calculations of H, Cl, Na, O, and S atoms on a Ni_{20} cluster.

Comparing the total energies of all clusters, we find that every atom adds ≈ 3.5 eV to the total cohesive energy of the system,

independent from the direction in which the cluster is extended. For Pt_2 we get a value of 3.63 eV, which should be compared to experimental values of 3.71 ± 0.16 eV (equilibrium vapor pressure measurements^{41,42}) and 3.14 ± 0.02 eV (resonant two-photon ionization spectroscopy⁴⁰). Figure 4 shows the total bond energy of the clusters with respect to the amount of atoms. The linear behavior is nearly independent of the direction in which the cluster is extended, leading to a slope of 3.48 eV for the surface bond energy per atom. This suggests that the surface energy is independent of the nature of the surface (for these convex clusters). This calculated surface energy of 3.48 eV/atom is only 59.5% of the experimental cohesive energy for bulk platinum of 5.85 eV.⁴³ Assuming that the surface and bulk energies are proportional to the average number of bonded atoms, this result would suggest that the average number of bonds for the cluster is 7.2. Indeed, the average number of bonds in the $Pt_{9.10.9}$ -cluster is 6.9, which is 57.5% of the value (12) for the bulk crystal. (For an atom in the (111) surface there are 9 bonds, while an atom in the 100 surface has 8 bonds.) This suggests that the surface and bulk energies are proportional to the average number of bonded atoms.

However, the average number of surface atoms per cluster (see Figure 4) changes continuously with size, and it is not clear to us why even our smallest clusters of only 2 and 3 atoms still show the 3.5 eV bond energy per added atom.

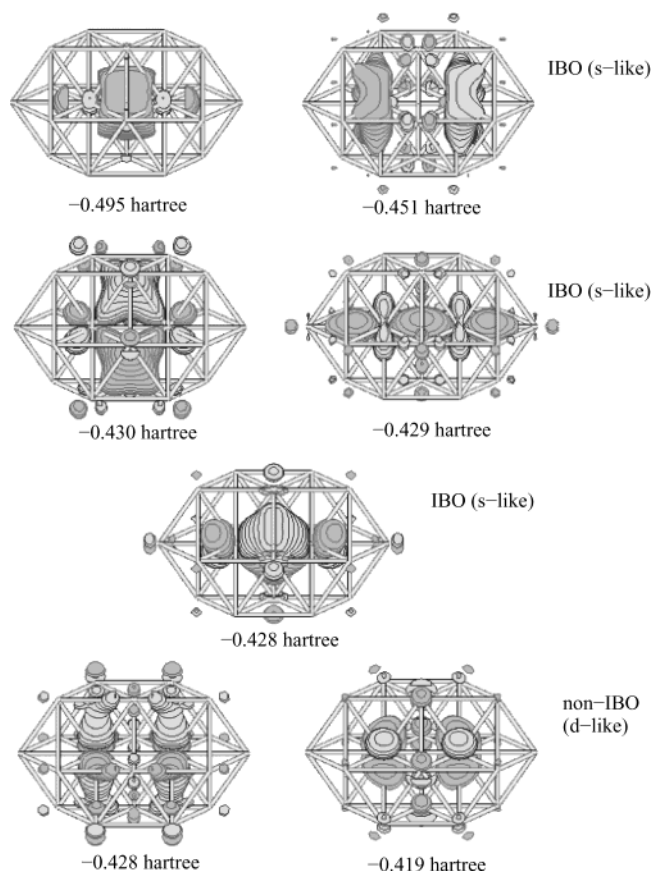
TABLE 1: Ground-State and Excitation Energies of the Different Pt-Clusters with Their Corresponding Spins. Listed Are All Excitation Energies of Spin-States near That of the Ground-State System

system	ground-state energy [hartree]	spin	excitation energy [eV]
Pt ₃	−357.402 19	1	0
		0	0.04 7
		2	0.69 7
Pt ₆	−714.917 24	3	0
		2	0.40 3
		1	0.72 2
		0	1.44 0
		4	1.65 3
Pt ₈	−953.257 35	3	0
		4	0.04 9
		2	0.75 2
Pt ₁₂	−1429.974 23	5	0
		6	0.00 6
		4	0.43 3
Pt _{6,3}	−1072.516 09	3	0.57 6
		4	0
		3	0.21 3
		2	0.64 8
		1	1.22 9
Pt _{8,4}	−1430.069 21	5	1.35 9
		5	0
		4	0.23 1
		3	0.27 5
		2	0.52 0
Pt _{12,7}	−2264.366 59	6	0.68 6
		6	0
		7	0.00 3
		5	0.12 7
		4	0.27 1
Pt _{5,10,5}	−2383.531 52	5	0
		3	0.10 9
		4	0.14 2
		2	0.38 9
		6	0.44 7
Pt _{9,10,9}	−3337.207 57	9	0
		8	0.14 1
		7	0.17 1
		6	0.22 4
		10	0.22 7

3.2. Adsorption of Oxygen. This section presents calculations of the chemisorption of atomic oxygen on Pt(111)-surface-clusters. We systematically examined the adsorption energy and the position of the oxygen on all different clusters of Figure 1. In each case, the adsorbate was located at one of the four possible positions:

- (i) *on-top* (η_1), with a surface Pt-atom directly under the adsorbate O atom,
- (ii) *bridge* (η_2), where the adsorbate O bridges two adjacent surface Pt-atoms,
- (iii) *fcc- η_3* , where the adsorbate O is above a 3-fold position in which there is no atom in the second surface-layer,
- (iv) *hcp- η_3* , where the adsorbate O is above a 3-fold position but there is a Pt-atom beneath the adsorbate in the second surface-layer.

Figure 5 shows these different adsorption sites for the Pt_{12,7}-cluster. For the single-layer clusters there is no geometric distinction between the fcc and hcp 3-fold positions. But because the IBOs prefer tetrahedra over octahedra for the two- and three-layer systems, we are able to distinguish between the triangles in the one-layer clusters. The tetrahedra formed by the first and second layer represent hcp sites on the surface, whereas the octahedra are associated with fcc sites. This leads to the following scheme for the planar systems: if there is an IBO

**Figure 3.** Seven lowest valence occupied orbitals of Pt_{5,10,5}.

located in the triangle, we consider it as a hcp site, otherwise the triangles are defined as fcc sites.

To calculate the adsorption energy and distance, we begin with an oxygen position consistent with the symmetry of the site. We then optimize the position of the oxygen so that the total energy is minimized, which allows one degree of freedom for the on-top position, two for the bridge site, and three for the fcc and hcp sites. Since the Pt(111)-surface shows nearly no relaxation,³³ the Pt-atoms are kept fixed at the bulk crystal geometry during the geometry optimization of the oxygen. For each bonding site, we will begin our discussion with the Pt_{9,10,9}-cluster, which we believe leads to converged results for each case. The interpretations on the bondings are based on the calculated bond length and the analysis of the net spin densities (Figure 7).

3.2.1. fcc 3-Fold Hollow Position (fcc- η_3). For the fcc site, there is no Pt-atom in the second layer under the adsorbate position. In calculations of this site, we first optimize the O position with the restriction that the distances to the three nearest Pt-atoms are equal. We then remove all restrictions for the adsorbate and reminimize. The results are given in Table 2. The Pt_{9,10,9}-cluster leads to a net bond energy of 3.28 eV. Since the oxygen atom has two unpaired spins, we expect to form two covalent bonds where each O orbital spin pairs with an unpaired d orbital on the metal to form a localized covalent bond. This would lead to a net decrease of the spin by one unit from that of the free cluster, and indeed, this is observed. After forming the two short covalent bonds (2.01 Å) directed at two of the Pt-atoms, there remains an O lone pair pointing at the other Pt-atom of the 3-fold hollow site. This suggests formation of a Lewis base–Lewis acid or donor–acceptor bond longer by

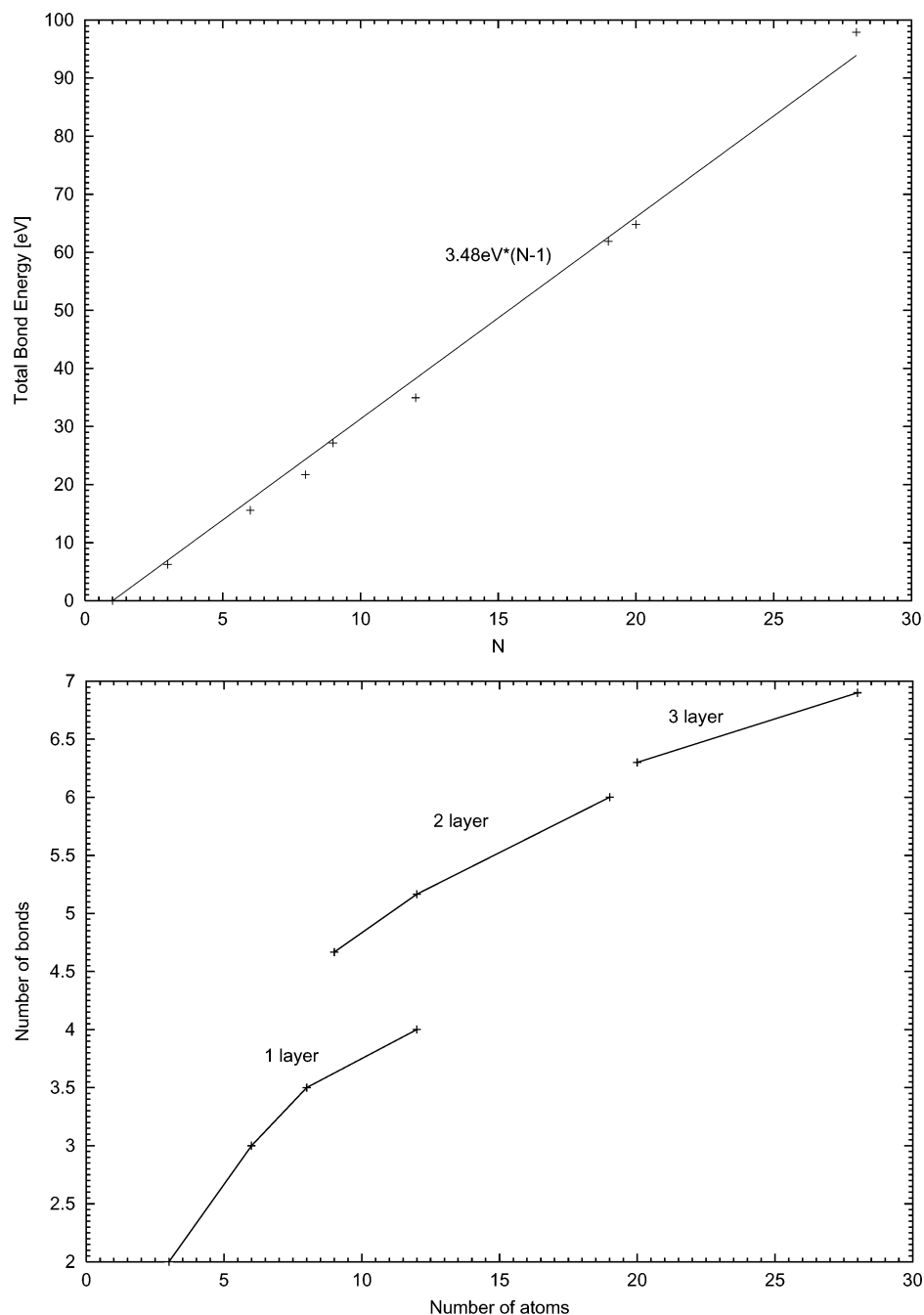


Figure 4. The upper diagram shows the total bond energy of the Pt-clusters versus the number of atoms. There is only little deviation from the linear dependency. In the lower plot, the average number of bonds of the different clusters versus the total number of atoms is shown. With increasing cluster size, the average number of bonds converges.

0.20 Å than the covalent single bond (see Figure 6). This difference of ≈ 0.2 Å between covalent bonds and donor–acceptor bonds has been observed previously.⁴⁴

To further analyze the bonding, we evaluated the unpaired spin density on the various atoms of this cluster with and without the oxygen. The results for the fcc site in Figure 7 suggest that the oxygen forms two covalent bonds to two Pt-atoms. The spin density located at the oxygen is nearly zero (0.16) and the spin density on atoms 3 and 4 (bonded to the O) is drastically reduced (from 0.64 to 0.34). For the longer bond to the third atom (7) the spin density changes little (0.64 to 0.68), denoting the Lewis base–Lewis acid or donor–acceptor nature of the bond. In addition, the projected spin for atoms 21 and 22 (located in the third layer below the adsorbate) changes significantly, probably reflecting the delocalization of the unpaired spin on the platinum

that spin couples to the oxygen and thereby reduces the spin density at these atoms. For all other atoms in the cluster, the oxygen induces only small deviations in the unpaired spin density.

The $\text{Pt}_{5,10,5}$ -cluster leads to two covalent bonds at 2.01 Å just as for $\text{Pt}_{9,10,9}$, but the donor–acceptor bond is only 0.09 Å longer than the covalent bonds, indicating that the small size (5 atoms in the first layer) of the surface cluster may have modified the bonding. Indeed, the net bond energy is 0.92 eV higher than for $\text{Pt}_{9,10,9}$. The bonding in this cluster might mimic the effect of a step edge near a binding site. Experimental studies on the adsorption of O_2 at Pt(111) step edges show an increased binding.^{45–47} In STM experiments, Ho and co-workers were able to detect O_2 on terrace sites up to 100 K. Above this temperature, some O_2 was desorbing and some was dissociating. For O_2 on

TABLE 2: Adsorption Energies and Distances for the Oxygen Atom at fcc Sites. Moreover, the Energies and Distances Are Given for Some Electronic Excitations^a

system	adsorption energy [eV]	spin	excitation [eV]	distance Pt–O [Å]	vibration freq. [cm ⁻¹]
Pt ₃	3.40 3	1	0	1.991	495
			0.38 1	2.100	
			0.58 3	1.990	
Pt ₆	2.68 4	1	0	1.924	562
			0.49 1	$a = 1.907, b = c = 2.052$	
			0.66 7	1.937	
Pt ₈	3.33 8	2	0	1.943	569
			0.49 0	2.015	
			0.60 3	1.952	
Pt ₁₂	3.31 9	4	0	1.949	589
			0.11 2	2.013	
			0.20 7	1.949	
Pt _{6,3}	2.08 9	2	0	2.024	650
			0.10 2	2.074	
			0.23 3	2.007	
Pt _{8,4}	2.39 0	3	0	$a = 2.120, b = c = 1.989$	461
			0.01 0	$a = 2.205, b = c = 2.007$	
			0.13 3	$a = 2.133, b = c = 1.980$	
Pt _{12,7}	2.94 1	6	0	$a = 1.965, b = c = 2.101$	477
			0.11 6	$a = 1.976, b = c = 2.060$	
			0.13 5	$a = 2.172, b = c = 2.074$	
Pt _{5,10,5}	4.20 8	4	0	$a = 2.096, b = c = 2.010$	559
			0.05 1	$a = 2.097, b = c = 2.005$	
			0.10 6	$a = 2.122, b = c = 1.997$	
Pt _{9,10,9}	3.28 4	8	0	$a = 2.207, b = c = 2.005$	510
			0.05 9	$a = 2.191, b = c = 2.059$	
			0.09 1	$a = 2.219, b = c = 2.003$	

^a If the distances of the oxygen to the three closest Pt-atoms are not equal within the error of the geometry optimization, all minor distances are listed, too. For the ground state, the vibrational frequencies of the adsorbate perpendicular to the Pt-surface are given.

step edges, they measured this transition to be at roughly 150 K, where at higher temperatures all the ad-molecules were desorbed.

The Pt_{12,7}-cluster might appear to be even better than Pt_{9,10,9} with 12 atoms in the top layer. However the ground state has a $S = 6$ just as the free cluster, suggesting that the O bonds to the excited state of the cluster (only 0.003 eV higher). Moreover it leads to one very short bond of 1.97 Å in addition to the two 2.10 Å bonds, indicating a different mode of bonding. The bonding in this system can be described by an electron transfer from the O lone pair orbital to the surface, allowing 3 covalent bonds. We believe that the problem with this and other two-layer clusters is that the presence of two adjacent surface planes leads to extra stabilization of some orbitals and destabilization of others. Thus, all two-layer clusters led to weaker bonds (by 0.34 to 1.2 eV).

On the other hand, the Pt₁₂- and Pt₈-planar clusters lead to bond energies within 0.03 and 0.05 eV of the Pt_{9,10,9} result, in agreement of the suggestion by KG that these would mimic the bulk binding. For these clusters, the spin decreases by one unit as expected for forming two covalent bonds, but the bonds are all equal and 0.12 Å shorter. The bonding here can again be described by an electron transfer from the O to the Pt-cluster, allowing three equivalent bonds. Note that we use the locations of the IBOs to assign a site as fcc. A site above an IBO is considered as hcp, and the fcc sites are the sites without an IBO contained in the triangle beneath.

Except for the small clusters Pt₃, Pt₆, and Pt_{6,3}, all ground-state spins are reduced by $\Delta S = 1$ compared to the clusters without adsorbate. Because there is no IBO at the fcc sites (fcc sites form octahedra and not tetrahedra), the bond is stronger than for the hcp site where there would be additional electron repulsion with the IBO.

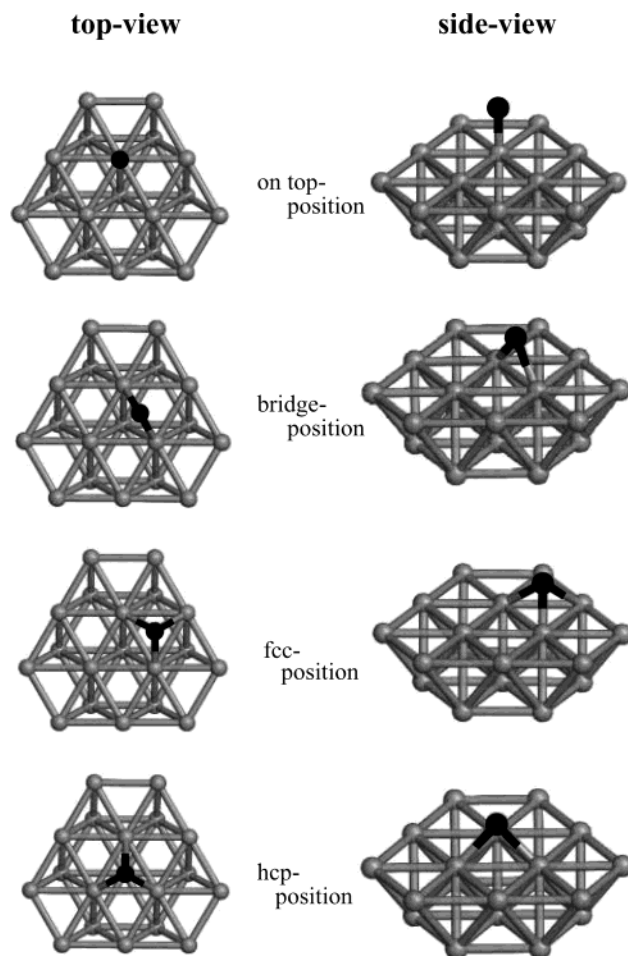


Figure 5. The different adsorption sites for oxygen are shown using the Pt_{12,7}-cluster as an example. The left pictures show the top-view on the surface and the right systems the side-view to the systems. In all pictures, the oxygen is black and the Pt atoms are gray.

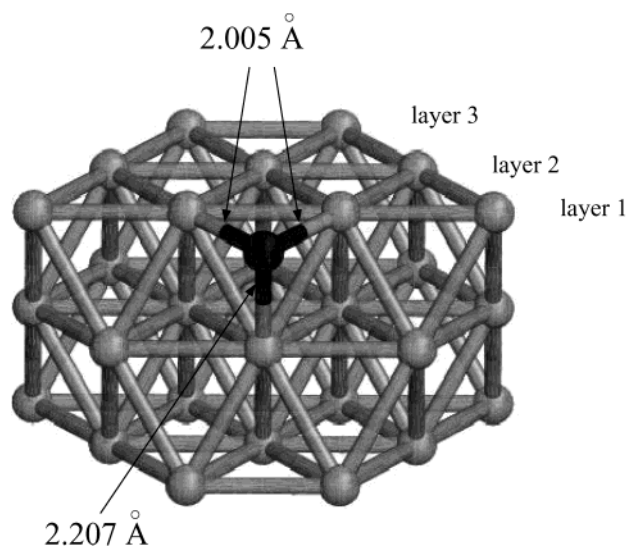


Figure 6. Adsorption on the Pt_{9,10,9}-cluster at the fcc site. The different bond lengths suggest that there are two covalent bonds (2.01 Å) and one donor–acceptor bond (2.21 Å).

The calculated vibrational frequencies fluctuate greatly for various clusters. We obtain the frequencies from the Hessian construction allowing just the O and the 3 bonded Pt-atoms to move (all other atoms were fixed). The result is a perpendicular vibration of 510 cm⁻¹ and parallel vibrations of 864 and 882

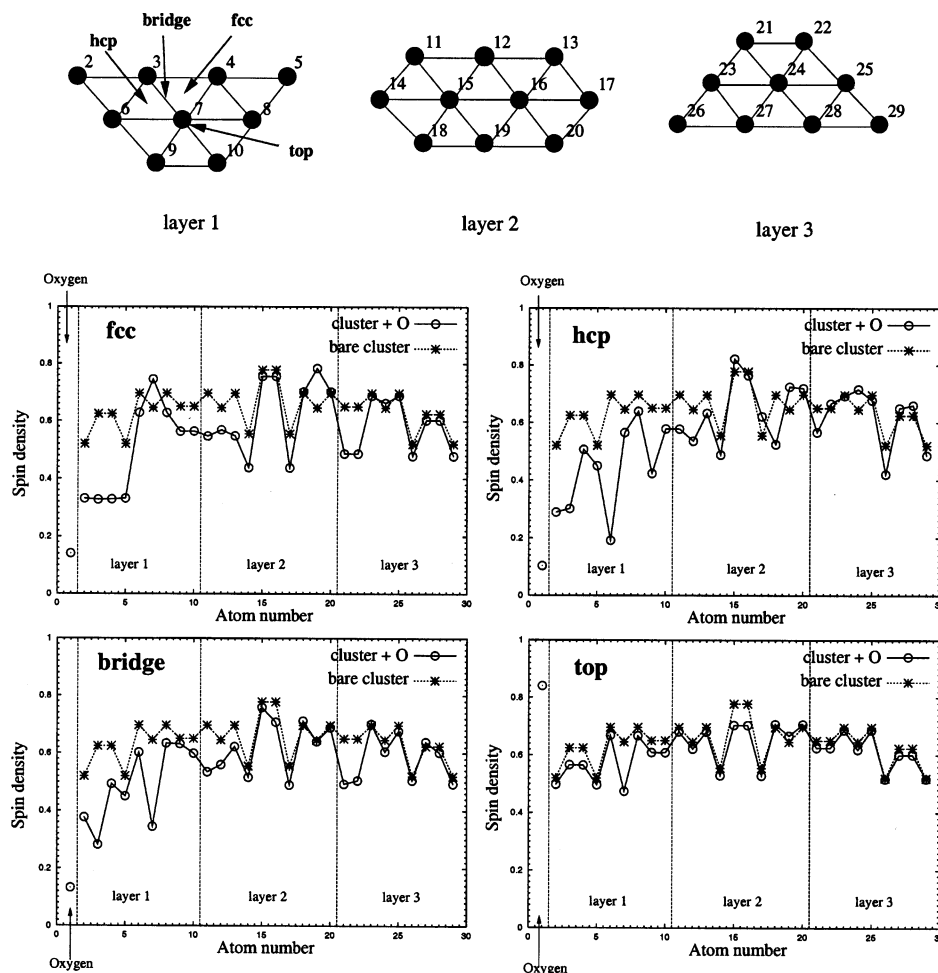


Figure 7. The upper part shows the numbering of the atoms for the different layers of the $\text{Pt}_{9,10,9}$ -cluster. Moreover, the different adsorption sites are drawn. The diagrams show the net spin density (see section 2) of the unpaired orbitals (based on the Mulliken population) for each atom according to the numbering above. Each of the four diagrams belongs to one adsorption site at the $\text{Pt}_{9,10,9}$ -cluster. For comparison, both the bare cluster and the cluster with oxygen are plotted. The different areas of the diagrams indicate the layers of the cluster and the oxygen adsorbate (atom 1 in all plots).

cm^{-1} , respectively. These frequencies may be compared to the experimental values on the $\text{Pt}(111)$ -surface of 466 to 480 cm^{-1} for the perpendicular vibration^{10,15–17} (no results for the parallel vibration have been reported; these would come from off-specular EELS). For smaller clusters, we also checked the vibrational frequencies of the oxygen atom by giving all Pt-atoms complete freedom; the deviation was only 1–3%.

For adsorption on the fcc site, Mulliken charge analysis leads to net electron charge at the oxygen of -0.55 e (see Table 6), suggesting reasonably high polarity of the Pt–O covalent bonds.

3.2.2. hcp 3-Fold Hollow Position ($\text{hcp}-\eta_3$). For the adsorption at the hcp site we use the same approach explained above. All results for clusters with hcp sites are given in Table 3.

The major difference between the hcp and fcc clusters is that hcp has an IBO localized just below the binding site. This presence may lead to unfavorable overlap effects with the new bonds at the surface. Thus for the $\text{Pt}_{9,10,9}$ -cluster, we obtain a bond energy 0.33 eV weaker than for fcc. Here the hcp geometry has two short bonds at 2.04 Å and one at 2.15 Å similar to the values obtained for the fcc site (2.01 and 2.21 Å). Just as for fcc, the $\text{Pt}_{5,10,5}$ leads to a greatly increased bond energy (by 1.2 eV), and the two layer clusters again lead to erratic results. Indeed, the $\text{Pt}_{12,7}$ -cluster puts the hcp site in the center of the surface-cluster, leading to an adsorption energy for the oxygen smaller than for the $\text{Pt}_{9,10,9}$ -cluster by only 0.14 eV. Furthermore, we find that the hcp results for the one-layer clusters are

erratic: the 8-atom system leads to two short bonds (1.95 Å), with the third bond 0.3 Å longer, whereas Pt_{12} leads to two bonds at 2.04 Å, with the third bond 0.1 Å shorter. For the $\text{Pt}_{9,10,9}$ - and $\text{Pt}_{5,10,5}$ -clusters, the bonding to the hcp sites appears very similar to that found for the fcc site. The total spin drops by 1 unit and the two short bonds and one longer bond again suggest two covalent and one donor–acceptor bond (see section 3.2.1). In addition, the net charge on the O is similar (-0.50 e for hcp and -0.55 e for fcc) (see Table 6), and for $\text{Pt}_{9,10,9}$ the spin-projection (see Figure 7) at the oxygen atom is small (0.18). However for hcp, bonding the O affects both the two Pt-atoms with the covalent bond (atoms 3 and 6) and the other two atoms (7,15) of the tetrahedra containing the IBO below the adsorption site.

In contrast, we find more erratic results for describing adsorption on the hcp site the smaller clusters: Pt_6 , Pt_8 , Pt_{12} , $\text{Pt}_{6,3}$, Pt_6 , and $\text{Pt}_{8,4}$. Here the spin change in the ground state is often zero, which suggests that the IBO at the tetrahedra under the hcp site can have a strong influence on the nature of the bonding to Pt.

3.2.3. Bridge Position (η_2). To obtain the adsorption energy and bond distance of the oxygen at the bridge position, the geometry was optimized under the restriction that the oxygen is allowed to move only in the plane perpendicular to the surface containing the two nearest surface Pt-atoms (the Pt–O distances are not constrained to be equal). Moreover we always locate

TABLE 3: Adsorption Energies and Distances for the Oxygen Atom at hcp Sites. Moreover, the Energies and Distances Are Given for Some Electronic Excitations^a

system	adsorption energy [eV]	spin	excitation [eV]	distance Pt–O [Å]	vibration freq. [cm ⁻¹]
Pt ₆	3.51 0	3	0	$a = 1.921, b = c = 2.142$	498
			0.03 8	$a = 2.214, b = c = 1.940$	
			0.30 3	1.944	
			1.31 8	2.158	
Pt ₈	3.65 4	3	0	$a = 2.259, b = c = 1.954$	499
			0.13 3	$a = 2.258, b = c = 1.927$	
			0.21 9	$a = 2.234, b = c = 2.055$	
			0	$a = 1.937, b = c = 2.041$	
Pt ₁₂	3.63 6	5	0	$a = 1.901, b = c = 1.979$	567
			0.01 8	$a = 1.906, b = c = 1.980$	
			0.34 2	$a = 1.906, b = c = 1.980$	
			0.25 3	$a = 1.906, b = c = 1.980$	
Pt _{6,3}	3.03 7	4	0	$a = b = 2.032, c = 2.248$	420
			0.14 8	$a = 1.926, b = c = 2.144$	
			0.28 6	$a = 1.934, b = c = 2.056$	
			0.83 2	$a = 2.081, b = c = 2.161$	
Pt _{8,4}	1.86 9	5	0	2.091	477
			0.13 2	2.054	
			0.24 9	2.042	
			0.30 3	2.016	
Pt _{12,7}	2.80 6	7	0	2.107	621
			0.04 1	2.050	
			0.10 4	2.076	
			0.62 2	2.121	
Pt _{5,10,5}	4.20 6	4	0	$a = 2.137, b = c = 2.021$	524
			0.07 1	2.039	
			0.09 4	$a = 1.990, b = c = 2.139$	
			0	$a = 2.149, b = c = 2.040$	
Pt _{9,10,9}	2.94 6	8	0	$a = 2.155, b = c = 2.031$	531
			0.05 2	$a = 2.201, b = c = 2.054$	
			0.10 2		

^a Because for Pt_{8,4} the completely free oxygen always moved out of the hcp-site, we listed the values for the restricted system where all three distances were kept equal. In all other cases, if the distances of the oxygen to the three closest Pt-atoms is not equal within the error of the geometry optimization, all distances are listed. For the ground state, the vibrational frequencies of the adsorbate perpendicular to the Pt-surface are given.

the adsorbate at the bridge site furthestmost from the borders of the cluster to minimize edge effects. All adsorption energies, bond distances, spin-states, and excitation energies for the lowest excited states of each spin multiplicity (only close to the spin multiplicity of the ground state) are given in Table 4.

The largest three-layer system (Pt_{9,10,9}) leads to a spin that is one unit lower than the bare cluster, suggesting that the O atom makes a covalent bond to each Pt-atom just as is found for the fcc and hcp sites and by KG for CH₂. The bridge site has an adsorption energy of 2.73 eV, which is 0.56 eV weaker than when the O is allowed to bend over and bond to a third Pt. This suggests that we consider the strength of the donor–acceptor bond as 0.56 eV, whereas the average covalent bond is 1.37 eV. Although the bond lengths of the two bonds for the bridge site (1.99 Å) increase by just 0.015 Å in going to the fcc site, the average covalent bond energy could be slightly less than 1.37 eV.

To further analyze the bonding, we consider the unpaired spin density on the various atoms of the cluster with and without the oxygen. Figure 7 indicates that, just as with the fcc and hcp sites, there is little net spin at the oxygen. The assumption that the oxygen at the bridge site makes two covalent bonds to unpaired d orbitals of the nearest atoms (3,7) is confirmed by drastic reduction of the projected spin (see section 2) for these atoms. For all other atoms, only minor changes are observed.

TABLE 4: Adsorption Energies and Distances for the Oxygen Atom at Bridge Sites. Moreover, the Energies and Distances for Some Electronic Excitations Are Given^a

system	adsorption energy [eV]	spin	excitation [eV]	distance Pt–O [Å]
Pt ₃	3.45 5	0	0	1.909
			0.18 6	1.921
			0.57 6	1.973
Pt ₆	2.63 7	2	0	1.927
			0.42 8	$a = 1.920, b = 2.162$
			0.44 1	1.921
Pt ₈	3.14 5	2	0	1.925
			0.28 5	1.934
			0.61 6	1.933
Pt ₁₂	2.84 2	5	0	1.943
			0.00 6	2.000
			0.28 1	1.934
Pt _{6,3}	2.17 8	3	0	1.988
			0.15 8	1.968
			0.38 3	2.037
Pt _{8,4}	2.13 3	3	0	1.982
			0.08 1	1.990
			0.12 5	1.982
Pt _{12,7}	2.67 0	6	0	2.001
			0.00 7	2.011
			0.07 5	1.979
Pt _{5,10,5}	3.79 7	4	0	1.978
			0.08 9	1.975
			0.15 4	1.976
Pt _{9,10,9}	2.72 9	8	0	1.990
			0.07 8	1.998
			0.09 0	1.978

^a If the distances of the oxygen to the two closest Pt-atoms is not equal within the error of the geometry optimization, both distances are listed.

Just as for the fcc and hcp sites, the electronic charge of the chemisorbed oxygen is about $-0.50 e$ (see Table 6).

As for the fcc and hcp sites, the Pt_{5,10,5}-cluster leads to a much larger bond energy (by 1.05 eV) although the bond distances decrease by only 0.01 Å. As with hcp, the largest two-layer cluster (Pt_{12,7}) leads to results close to the Pt_{9,10,9}-cluster (0.05 eV weaker), but the smaller two-layer clusters lead to much weaker binding. The 12-atom planar cluster leads to a bond energy only 0.12 eV stronger than the largest cluster, but the bond distances are 0.05 Å smaller, just as for the other sites.

The adsorption energy is more sensitive to the size and shape of the cluster than the distances are. This suggests that the energies and locations of the cluster orbitals play an important role in the bonding. The two-layer clusters with 6 and 8 atoms in the first layer are too small to describe the chemisorbed state sufficiently. The energies for adsorption on Pt_{6,3} and Pt_{8,4} indicate convergence with respect to cluster size. However, the results for Pt_{12,7} show that this correspondence is only because both clusters have similar structure at the bridge adsorption site.

In all cases except Pt₁₂ and Pt_{12,7}, the ground-state spin is reduced by $\Delta S = 1$ from the clusters without an adsorbate. Indeed, keeping in mind the discussion of section 3.1 for the ground-state spins of the bare Pt₁₂- and Pt_{12,7}-clusters, we can consider that there is no exception. As mentioned above, this suggests that the bonding is covalent with two unpaired spins of the O spin-pairing to two singly occupied d orbitals on adjacent Pt-atoms.

In summary, the bridge-site adsorption is well described by the Pt₁₂-, Pt_{12,7}-, and Pt_{9,10,9}-clusters.

3.2.4. On-Top Position (η_1). To keep the adsorbate in the on-top position, we constrained the O atom to move only in

TABLE 5: Adsorption Energies and Distances for the Oxygen Atom on Top of the Different Systems^a

system	adsorption energy [eV]	spin	excitation energy [eV]	distance Pt–O [Å]
Pt ₃	2.81 2	1	0	1.793
		2	0.24 1	1.813
		3	1.09 0	1.813
		0	1.33 2	1.777
Pt ₈	1.90 7	4	0	1.860
		3	0.05 7	1.802
		2	0.26 6	1.840
		1	0.82 4	1.837
		5	0.89 7	1.796
Pt ₁₂	1.96 4	5	0	1.829
		6	0.02 8	1.847
		4	0.31 9	1.821
Pt _{8,4}	2.15 7	5	0	1.828
		4	0.00 8	1.828
		3	0.27 7	1.830
		2	0.41 7	1.926
		6	0.70 2	1.824
Pt _{12,7}	2.36 0	7	0	1.840
		6	0.12 9	1.832
		5	0.27 1	1.831
		8	0.40 0	1.844
Pt _{5,10.5}	3.06 2	6	0	1.829
		7	0.10 7	1.831
		8	0.24 9	1.828
Pt _{9,10.9}	2.01 5	5	0.30 9	1.832
		9	0	1.872
		8	0.16 5	1.846
		10	0.21 1	1.894

^a Moreover, the energies and distances for some electronic excitations are given. The adsorption on the Pt_{6,3}-cluster is not considered because all on-top sites are directly at the edges.

the direction perpendicular to the surface during geometry optimization. Table 5 shows the results for the adsorption at the on-top site.

For the Pt_{9,10.9}-cluster, the bond energy is 2.01 eV, which is considerably weaker than the η_2 (bridge) and η_3 (3-fold) sites. The spin-state is the same as that of the bare cluster, indicating that a p singly occupied orbital of the O has spin paired to a d singly occupied orbital on the cluster, leading to one unpaired spin on the O (π with respect to the bond). The result is no net change in the spin. The bond distance of 1.87 Å is 0.12 Å shorter than even the bridge bond, and 0.13 Å longer than the bond in the diatomic Pt–O molecule. For the bridge binding, where O uses the two unpaired spins to make a bond to each of the two closest Pt-atoms, we consider the bond order to be 1. However, for the Pt–O molecule, the bond order is 2 (analogous to O₂). Since the on-top binding on Pt_{9,10.9} led to a bond distance that is half between these both cases, we conclude a bond order of 1.5 for the on-top binding.

Comparing the unpaired spin density on the various atoms of the cluster with and without the oxygen (Figure 7), we find results dramatically different than for the other three adsorption sites. Here the net spin of the oxygen is 0.82 (5 times the value for the other cases). The only Pt spin density that changes for the on-top site is the Pt-atom (7) directly below the adsorbate, with essentially no change in the spin density of all other atoms. This confirms the description of the bonding given above. The σ singly occupied p orbital of the oxygen spin pairs with one singly occupied Pt d orbital, leaving a singly occupied p- π orbital on the oxygen. The on-top bonding has the smallest effect on all other atoms of the cluster, indicating a strongly localized bond. The difference in bond strength of 0.71 eV between the on-top bond (2.02 eV) and the bridge bond (2.73 eV) can be

TABLE 6: Summary of the Calculated Charge Transfer to the Oxygen Adsorbate, Adsorption Energies, Bond Distances, and Vibrational Frequencies at Different Sites (based on Pt_{9,10.9})

	on-top	bridge	hcp	fcc	expt. ^a	slab ^b
<i>Q</i> (oxygen) [e]	−0.38	−0.50	−0.50	−0.55		
<i>E</i> [eV]	2.01 5	2.72 9	2.94 6	3.28 4	3.47–3.73	3.43
<i>R</i> _{Pt–O} [Å]	1.872	1.990	2.040	2.005	2.01 ± 0.05	2.02
ω [cm ^{−1}]			531	510	466–480	470

^a Parker et al., ref 16, TPD experiments, ads. energies for 0–0.25 ML coverage (see section 3.3). ^b Eichler et al., ref 20, spin-polarized DFT slab calculations (GGA gradient-corrected xc-functional, ultrasoft pseudopotential).

thought of in terms of the strain in forming the Pt–O–Pt three-membered ring of the bridge bond, which increases the bond length by 0.12 Å and decreases the bond energy by 2.02 – 0.71 = 1.31 eV = 30 kcal/mol over simple bond additivity. This is amazingly close to the value of 26 kcal/mol deduced for the strain in the three-membered ring of cyclopropane.⁴⁸

Just as for the other adsorption sites the bonding for the Pt_{5,10.5}-cluster is 1.05 eV higher. The chemisorption on both two-layer clusters lead to similar bond distances but erratic bond energies. The chemisorption on Pt₁₂ and Pt₈ give bond energies just 0.05 eV and 0.11 eV weaker than for Pt_{9,10.0}, indicating again the validity of using these simple clusters. For O–Pt₈ the spin-state was calculated to be *S* = 4 (8 unpaired spins), whereas it was *S* = 3 (6 unpaired spins) for the bare cluster (without adsorbate), which is compatible with the neutral-Lewis model. However, a spin state of *S* = 3 for O–Pt₈ (oxygen causes no net change in the spin) would be compatible with the covalent model. Indeed, this state is only 0.06 eV higher than the *S* = 4 state. The largest one-layer system considered has 12 atoms, which leads to a change in the chemisorption energy of less than 0.06 eV and a change in the bond distance of \approx 0.03 Å compared to O–Pt₈. This again suggests that the bond is quite localized. Here, the spin state of the system with adsorbate is *S* = 7 compared to *S* = 6 for the bare cluster. But because for the bare cluster the *S* = 7 state is only 0.003 eV higher, this is also compatible with the covalent model.

The introduction of a second layer increases the adsorption energy by 0.25 eV to 2.16 eV for Pt_{8,4} and to 2.36 eV for Pt_{12,7}. For both cases, the change in bond distance is only \approx 0.01 Å. As for the planar clusters, the ground-state spin did not change upon chemisorption. Indeed, on-top adsorption of the oxygen did not change the ground-state spin for nearly all clusters (one-, two-, or three-layers). Thus, all on-top sites appear to have covalent bonding with a π -unpaired spin bond on the oxygen.

Considering clusters with more than 5 atoms in the first layer, there is a trend for the adsorption energy with respect to the direction in which the cluster is extended. Comparing Pt₈ with Pt₁₂ and Pt_{8,4} with Pt_{12,7} shows that an extension in lateral direction fortifies the bond. This indicates the delocalization of the surface electrons. The same can be observed for the introduction of the second layer: compare Pt₈ with Pt_{8,4} and Pt₁₂ with Pt_{12,7}. However, including a third layer causes a decrease in adsorption energy: compare Pt_{8,4} with Pt_{9,10.9}.

The Mulliken analysis of the on-top adsorbed oxygen gives a charge of −0.38 e (see Table 6). This behavior is different compared to the other adsorption sites where the oxygen is charged by \approx −0.50 e.

3.3. Comparison to Experiment. Good experimental data for comparison exists only for single-crystal extended surfaces. We will compare these experimental results only to the calculations for Pt_{9,10.9}. The STM experiments of Ho^{45–47} show

quite clearly that O binds to an η_3 site, and Ho has concluded that this site is the fcc site. His studies find no evidence for bridging or on-top sites or for the η_3 hcp site. This is consistent with our results, which find these other sites to be at least 0.33 eV higher in energy.

Experimental data on the binding energy for chemisorbed atomic oxygen on the Pt(111)-surface were given by Parker et al.¹⁶ From temperature-programmed desorption (TPD) experiments they obtain the following values for the recombination barrier of adsorbed atomic oxygen to desorbed O₂: 1.73 eV (0.25 ML coverage) and 2.21 eV (zero coverage limit). Together with the experimental O₂ bond energy of 5.21 eV⁴⁹ (our calculations: 5.32 eV), their results lead to a surface bond energy of 3.47 eV for 0.25 ML coverage and 3.71 eV for the zero coverage limit. Since our cluster is a finite system, which still shows border effects, we assume that our calculated bond energy (3.28 eV) corresponds to low coverages (0–0.25 ML).

The optimum geometry of the O to the surface shows two bond distances of 2.01 Å and one of 2.21 Å. This corresponds to a surface–O distance of 1.307 Å and a displacement of 0.18 Å from the center of the surface triangle. The distance to the closest Pt-atoms of 2.01 Å is in agreement with the LEED experiments of Materer et al.¹⁷ who obtain 2.02 Å. There is no experimental evidence of the 0.18 Å lateral shift, but the resolution of the experiments is not yet adequate to detect such a small shift.

3.4. Comparison to Previous Calculations. (i) *Cluster Studies.* Previous DFT calculations (STO-basis, B88/P86 gradient-corrected density functional) on the O–Pt(111) chemisorption have been reported by Fahmi et al.¹³ They used Pt₄ and Pt₈ single-layer clusters and calculated 2.82 eV for the chemisorption on the η_3 site. Since our six-atom cluster has comparable size, their value can be compared to our result of 2.68 eV with Pt₆ (central η_3 site). Studies by Chen et al.¹⁴ used the same approach with a Pt_{6,3,1}-cluster that led to 2.86 eV for the η_3 site. This system should be compared with our Pt_{6,3}-cluster (bond energy: 2.08 eV) plus additional effects caused by the third layer atom. But our results show the introduction of a third layer leads to stronger bonds. On the basis of our results, none of the previously mentioned calculations are expected to yield consistent conclusions for all adsorption sites of the Pt(111)-surface.

Another interesting aspect is the transition of Pt between molecule and metal. Performing ab initio SCF/MP2 calculations, Xu² analyzed the changes in the density of states (DOS) with respect to the cluster size. For systems ≥ 7 Pt-atoms, he found no significant changes in the DOS and interpreted this as a transition to metallic properties. However, our results suggest that clusters of ≈ 28 atoms might be required for an accurate surface description.

(ii) *Periodic Slabs.* Calculations have been reported for chemisorption of O atom on periodic slabs by Feibelman et al.¹⁸ Using DFT within the LDA-approximation for the exchange-correlation, they found that oxygen prefers the fcc sites with an O–Pt bond distance of 2.00 Å and a bond energy of 5.28 eV, with the hcp site 0.33 eV higher. Their result for the bond distance agrees well with our value of 2.01 Å, but their bond energy is 50% larger. This is consistent with many other studies which show that the LDA-approximation leads to reasonable geometries but severely overestimates binding energies. However, the difference between the binding energies of the hcp and fcc sites agrees well with our value of 0.34 eV. Similar LDA studies by Bleakley and Hu¹⁹ lead to 4.43 eV and 2.02 Å for the oxygen binding at the fcc site. More recent spin-polarized DFT calculations by Eichler et al.²⁰ using the PW91 GGA

exchange-correlation functional found a recombination barrier from two adsorbed O atoms to a desorbed O₂ molecule of 1.65 eV at the fcc site and 0.98 eV at the hcp site. That leads to a difference between both sites of about 0.34 eV per atom, in agreement with our value. Using the experimental bond energy of 5.21 eV for O₂, their results lead to an adsorption energy of 3.43 eV (0.5 ML) for a single atom, which is only 0.15 eV above our value.

4. Summary

This paper presents calculations to determine the best cluster model for describing adsorption processes on the Pt(111)-surface. We considered the energetics and spin states for a variety of cluster sizes and shapes.

(1) Bond energy and bond distance. We find that Pt_{9,10,9} is the smallest cluster suitable for describing all four binding sites: η_3 -fcc, η_3 -hcp, η_2 , and η_1 . The results calculated with this cluster are in good agreement with experimental results on this surface and with the best calculations on periodically infinite slabs. Thus, all results agree that the η_3 -fcc site is favored with a bond distance of ≈ 2.01 Å. In addition, our calculated bond energy of 3.28 eV is consistent with the experimental values for low coverages (3.47 to 3.71 eV) and with the best DFT calculations on a surface (3.43 eV).

(2) Interpretation in terms of the interstitial electron model (IEM). We find that the ground-state spin and electronic structure of the different clusters can be explained quite well in terms of the IEM. According to IEM there are doubly occupied interstitial orbitals in various tetrahedra (or alternate triangles for planar clusters). We interpret the suitability of a cluster in terms of the IEM in which the surface IBO tends to be in tetrahedral sites having three Pt on the surface and the third Pt in the second layer. Moreover, the bonding of O to the η_3 sites (both fcc and hcp) are interpreted in terms of the IEM localized covalent bonding model, in which the two singly occupied orbitals of O bond to singly occupied d orbitals of Pt, while the lone pair of p orbitals on the O coordinates to the third Pt of an η_3 site to form a donor–acceptor bond. This leads to two bonds of 2.01 Å and one of 2.21 Å. However, this behavior could also be due to the different symmetry of the 3-fold positions. For example, the fcc site of Pt₁₂ is the central triangle (according to the IEM-prediction of section 3.1) for which we found three equivalent (but short) bonds, whereas the Pt_{12,7}-system where the fcc site is adjacent to the central triangle leads to one short and two longer bonds.

Our interpretation that the Pt_{9,10,9}-cluster is best, because it allows the IBO containing tetrahedra to terminate at the surface, suggests that to obtain truly converged results might require either the Pt_{9,10,10,9}-cluster which should have 9 IBOs between both layers 1 and 2 and between layers 3 and 4, or even better the Pt_{9,10,10,10,9}-cluster which in addition to these 9 + 9 IBOs could also have more bulk like IBOs involving the middle layer. This system would also have an odd number of layers, which is consistent with our findings that odd-numbered systems are superior to even-numbered systems.

(3) Other clusters. For the 2-layer models the IEM implies that the second layer must have more atoms than the top layer. Thus the Pt_{12,7}-cluster is appropriate for bonding to the seven-atomic surface but not the 12-atomic surface. The Pt_{5,10,5}-cluster gives bond energies about 1 eV too high for all binding sites. This is because the five-atom surface is dominated by edge effects, but this may model the bonding at step edges or kink sites. Our analysis suggests that the single-plane models can be unsuitable, but we find that the Pt₁₂-cluster gives excellent

bond energies for 3 types of sites (the exception is η_3 -hcp). However the bond distances for the single-plane structure are systematically low by ≈ 0.05 Å.

(4) Ground-state spin. The IEM successfully predicts the changes in the ground-state spins from cluster to cluster and upon adsorption of O. For adsorption on top-, bridge-, hcp-, and fcc sites it predicts a reduction of $\Delta S = 1$. Our results on the largest clusters show exactly this behavior.

To describe the bond distances sufficiently, we conclude that the second-nearest neighbors around the adsorption site are required. This leads to about 8–12 atoms in the first layer. For on-top and fcc sites, the introduction of a second layer makes the description worse. Therefore one should use either one- or three-layer systems for these adsorption sites. Different is the behavior for the oxygen adsorption at hcp or bridge sites, both of which require two or more layer Pt-clusters. Since the inclusion of a fourth layer has only a minor influence on the adsorption,^{50,51} we conclude that the three-layer system Pt_{9,10,9} is the most sufficient simple structure for describing adsorption processes on the Pt(111)-surface. The adsorption energies, bond distances, and vibrational frequencies predicted for the different sites are summarized in Table 6. The comparison of the experimental results with our calculated values shows good agreement for the bond distance and vibrational frequency. The calculated binding energies are consistent with the best experimental values.

5. Conclusion

We chose to study the adsorption of an oxygen atom on all possible sites of Pt-clusters, both because it is important in electrochemical reduction of O₂ and because it should place strong demands on the cluster. Thus, a cluster model of the surface that can describe the adsorption of atomic oxygen should also be sufficient for the less-reactive O₂ molecule and other simple molecules on the Pt(111)-surface. Our conclusion is that Pt_{9,10,9} is the smallest adequate cluster. We find that this cluster gives results within the experimental errors for the geometry and bond energies and that it agrees within computational accuracy with the best calculations on periodic slabs.

Acknowledgment. T.J. gratefully acknowledges support by the German academic exchange service (DAAD). This work was also supported by General Motors. The computation facilities of the MSC have been supported by grants from DURIP, NSF (MRI, CHE), and IBM-SUR. In addition, the MSC is supported by grants from DOE ASCI ASAP, ARO-MURI, NIH, ONR, ChevronTexaco, Beckman Institute, Seiko-Epson, Asahi Kasei, Avery-Dennison, Kellogg's, and 3M.

References and Notes

- (1) Akinaga, Y.; Tagetsugu, T.; Hirao, K. *J. Chem. Phys.* **1997**, *107*, 415.
- (2) Xu, W.; Shierbaum, K. D.; Goepel, W. *Int. J. Quantum Chem.* **1997**, *62*, 427.
- (3) Li, T.; Balbuena, P. B. *J. Phys. Chem. B* **2001**, *105*, 9943.
- (4) Anderson, A. B.; Grantscharova, E. *J. Phys. Chem.* **1995**, *99*, 9143.
- (5) Anderson, A. B.; Grantscharova, E. *J. Phys. Chem.* **1995**, *99*, 9149.
- (6) Kua, J.; Faglioni, F.; Goddard, W. A., III. *J. Am. Chem. Soc.* **2000**, *122*, 2309.
- (7) McAdon, M. H.; Goddard, W. A., III. *Phys. Rev. Lett.* **1985**, *55*, 2563.
- (8) Kua, J.; Goddard, W. A., III. *J. Phys. Chem. B* **1998**, *102* (47), 9481, 9492.
- (9) Campbell, C. T.; Ertl, G.; Kuipers, H.; Segner, J. *J. Chem. Phys.* **1980**, *73*, 5863.
- (10) Gland, J. L.; Sexton, B. A.; Fisher, G. B. *Surf. Sci.* **1980**, *95*, 587.
- (11) Campbell, C. T.; Ertl, G.; Kuipers, H.; Segner, J. *Surf. Sci.* **1981**, *107*, 220.
- (12) Yeo, Y. Y.; Vattuone, L.; King, D. A. *J. Chem. Phys.* **1997**, *106*, 392.
- (13) Fahmi, A.; van Santen, R. A. *Z. Phys. Chem.* **1996**, *197*, 203.
- (14) Chen, M.; Bates, S. P.; van Santen, R. A.; Friend, C. M. *J. Phys. Chem. B* **1997**, *101*, 10051.
- (15) Steininger, H.; Lehwald, S.; Ibach, H. *Surf. Sci.* **1982**, *17*, 342.
- (16) Parker, D. H.; Bartram, M. E.; Koel, B. E. *Surf. Sci.* **1989**, *217*, 489.
- (17) Materer, N.; Starke, U.; Barbieri, A.; Döll, R.; Heinz, K.; van Hove, M. A.; Somorjai, G. A. *Surf. Sci.* **1995**, *325*, 207.
- (18) Feibelman, P. J.; Esch, S.; Michely, T. *Phys. Rev. Lett.* **1996**, *77* (11), 2257.
- (19) Bleakley, K.; Hu, P. *J. Am. Chem. Soc.* **1999**, *121*, 7644.
- (20) Eichler, A.; Mittendorfer, F.; Hafner, J. *Phys. Rev. B* **2000**, *62* (7), 4744.
- (21) Becke, A. D. *J. Chem. Phys.* **1993**, *98* (7), 5648.
- (22) Lee, C.; Yang, W.; Parr, R. G. *Phys. Rev. B* **1988**, *37*, 785.
- (23) Slater, J. C. *Quantum Theory of Molecules and Solids, Vol. 4: The Self-Consistent Field for Molecules and Solids*; McGraw-Hill: New York, 1974.
- (24) Becke, A. D. *Phys. Rev. A* **1988**, *38*, 3098.
- (25) Vosko, S. H.; Wilk, L.; Nusair, M. *Can. J. Phys.* **1980**, *58*, 1200.
- (26) Xu, X.; Goddard, W. A., III. *Phys. Rev. Lett.*, in press.
- (27) *Jaguar 4.2*; Schrödinger Inc.: Portland, OR, 2000.
- (28) Hay, P. J.; Wadt, W. R. *J. Phys. Chem.* **1985**, *82*, 299.
- (29) Goddard, W. A., III. *Phys. Rev.* **1968**, *174*, 659.
- (30) Kahn, L. R.; Goddard, W. A., III. *J. Chem. Phys.* **1972**, *56*, 2685.
- (31) Melius, C. F.; Olafson, B. D.; Goddard, W. A., III. *Chem. Phys. Lett.* **1974**, *28*, 457.
- (32) Melius, C. F.; Goddard, W. A., III. *Phys. Rev. A* **1974**, *10*, 1528.
- (33) Kittel, Ch. *Einführung in die Festkörperphysik*; R. Oldenbourg Verlag: München, 1991.
- (34) Majumdar, D.; Dingguo, D.; Balasubramanian, K. *J. Chem. Phys.* **2000**, *113* (18), 7922.
- (35) Pandya, R. K.; Joshi, K. B.; Jain, R.; Ahuja, B. L.; Sharma, B. K. *Phys. Status Solidi B* **1997**, *200*, 137.
- (36) Melius, C. F.; Upton, T. H.; Goddard, W. A., III. *Solid State Commun.* **1978**, *28*, 501.
- (37) Upton, T. H.; Goddard, W. A., III.; Melius, C. F. *J. Vac. Sci. Technol.* **1979**, *16*, 531.
- (38) Upton, T. H.; Goddard, W. A., III. *Phys. Rev. Lett.* **1979**, *42*, 472.
- (39) Upton, T. H.; Goddard, W. A., III. *CRC Crit. Rev. Solid State Mater. Sci.* **1981**, *10*, 261.
- (40) Taylor, S.; Lemire, G. W.; Hamrick, Y. M.; Fu, Z.; Morse, M. D. *J. Chem. Phys.* **1988**, *89* (9), 5517.
- (41) Gupta, S. K.; Nappi, B. M.; Gingerich, K. A. *Inorg. Chem.* **1981**, *20*, 966.
- (42) Morse, M. D. *Chem. Rev.* **1986**, *86*, 1049.
- (43) Lide, D. R. *Handbook of Chemistry and Physics*, 71st ed.; CRC Press: Boca Raton, FL, 1990–1991.
- (44) Ramachandran, S.; Tsai, B.-L.; Blanco, M.; Chen, H.; Tang, Y.; Goddard, W. A., III. *J. Phys. Chem.* **1997**, *101*, 83.
- (45) Stipe, B. C.; Rezaei, M. A.; Ho, W.; Gao, S.; Persson, M.; Lundquist, B. I. *Phys. Rev. Lett.* **1997**, *78* (23), 4410.
- (46) Ho, W. *Acc. Chem. Res.* **1998**, *31* (9), 567.
- (47) Ho, W. *Science* **1998**, *279*, 1907.
- (48) Benson, S. W. *Thermochemical Kinetics: Methods for the Estimation of Thermochemical Data and Rate Parameters*, 2nd ed.; John Wiley & Sons: New York, 1976.
- (49) Huber, K. P.; Herzberg, G. *Molecular Spectra and Molecular Structure: IV. Constants of Diatomic Molecules*; van Nostrand Reinhold Company: New York, 1979.
- (50) Jacob, T.; Geschke, D.; Fritzsche, S.; Sepp, W.-D.; Fricke, B.; Anton, J.; Varga, S. *Surf. Sci.* **2001**, *486* (3), 194.
- (51) Jacob, T.; Fritzsche, S.; Sepp, W.-D.; Fricke, B.; Anton, J. *Phys. Lett. A* **2002**, *300*, 71.